

3317
31P

**NASA
Technical
Memorandum**

NASA TM-108439

**INTER-COMPARISON OF WILDFIRE AND HIGH-
RESOLUTION INTERFEROMETER SOUNDER (HIS)
DATA FROM STORM-FEST: AN INVESTIGATION
OF WILDFIRE SPECTRAL CHANNEL DISCREPANCIES**

By G. J. Jedlovec and G. S. Carlson

**Space Sciences Laboratory
Science and Engineering Directorate**

March 1994

(NASA-TM-108439) INTER-COMPARISON
OF WILDFIRE AND HIGH-RESOLUTION
INTERFEROMETER SOUNDER (HIS) DATA
FROM STORM-FEST: AN INVESTIGATION
OF WILDFIRE SPECTRAL CHANNEL
DISCREPANCIES (NASA, Marshall
Space Flight Center) 31 p

N94-29553

Unclas

G3/43 0003817



National Aeronautics and
Space Administration

George C. Marshall Space Flight Center

REPORT DOCUMENTATION PAGE

Form Approved
OMB No. 0704-0188

Public reporting burden for this collection of information is estimated to average 1 hour per response, including the time for reviewing instructions, searching existing data sources, gathering and maintaining the data needed, and completing and reviewing the collection of information. Send comments regarding this burden estimate or any other aspect of this collection of information, including suggestions for reducing this burden, to Washington Headquarters Services, Directorate for Information Operations and Reports, 1215 Jefferson Davis Highway, Suite 1204, Arlington, VA 22202-4302, and to the Office of Management and Budget, Paperwork Reduction Project (0704-0188), Washington, DC 20503.

1. AGENCY USE ONLY (Leave blank)		2. REPORT DATE March 1994	3. REPORT TYPE AND DATES COVERED Technical Memorandum	
4. TITLE AND SUBTITLE Inter-Comparison of Wildfire and High-Resolution Interferometer Sounder (HIS) Data from STORM-FEST: An Investigation of Wildfire Spectral Channel Discrepancies			5. FUNDING NUMBERS	
6. AUTHOR(S) G. J. Jedlovec and G. S. Carlson*				
7. PERFORMING ORGANIZATION NAME(S) AND ADDRESS(ES) George C. Marshall Space Flight Center Marshall Space Flight Center, AL 35812			8. PERFORMING ORGANIZATION REPORT NUMBER	
9. SPONSORING / MONITORING AGENCY NAME(S) AND ADDRESS(ES) National Aeronautics and Space Administration Washington, D.C. 20546			10. SPONSORING / MONITORING AGENCY REPORT NUMBER NASA TM-108439	
11. SUPPLEMENTARY NOTES *Universities Space Research Association Prepared by the Earth Science & Applications Division, Space Science Laboratory, Science and Engineering Directorate.				
12a. DISTRIBUTION / AVAILABILITY STATEMENT Unclassified--Unlimited			12b. DISTRIBUTION CODE	
13. ABSTRACT (Maximum 200 words) This simultaneous collection of HIS spectral measurements aboard the ER-2 during STORM-FEST provided a means to explore calibration problems in the infrared bands of the Wildfire instrument. Large discrepancies in brightness temperatures were noted in Wildfire bands designed to sample the "wings" of the strong ozone absorption band centered at 9.6 μm , where the atmospheric transmittance changes rapidly with wavelength. Examination of inter-channel relationships in Wildfire data and subsequent comparison to Wildfire data synthesized from the HIS measurements suggests that a wavelength shift in the channel spectral response from those determined in the laboratory may have occurred. Based on comparisons from several flights, this spectral shift has been empirically determined to be about 0.15 μm . It is speculated that this problem resulted from a slight misalignment of the spectrometer grating or other optical elements, or was a result of extreme range in temperatures experienced by the instrument throughout the course of an ER-2 flight. A consequence of this temperature fluctuation may be a change in a position of the grating in the optical path and could result in the variations in channel spectral response during flight. These findings for Wildfire may have significant bearing on future use of the MAS because of the similarities to the original Wildfire configuration.				
14. SUBJECT TERMS STORM-FEST, Wildfire, HIS, MAS, Spectral Shift, Diffraction Grating			15. NUMBER OF PAGES 31	
			16. PRICE CODE NTIS	
17. SECURITY CLASSIFICATION OF REPORT Unclassified	18. SECURITY CLASSIFICATION OF THIS PAGE Unclassified	19. SECURITY CLASSIFICATION OF ABSTRACT Unclassified	20. LIMITATION OF ABSTRACT Unlimited	

TABLE OF CONTENTS

	Page
I. INTRODUCTION	1
A. Motivation for the Report	1
B. Understanding the Data and the Problem.....	5
II. AIRCRAFT FLIGHTS AND INSTRUMENTATION.....	9
A. ER-2 Flights for STORM-FEST.....	9
B. Wildfire	11
C. High-Resolution Interferometer Sounder (HIS).....	13
D. Calibration of Wildfire Data	14
III. DATA COMPARISON	16
A. Wildfire and HIS Data	16
B. Inter-Comparison Results.....	18
IV. CONCLUSION.....	22
REFERENCES.....	24

PRECEDING PAGE BLANK NOT FILMED

LIST OF TABLES

No.	Title	Page
1	Selected Wildfire Channels for STORM-FEST.....	3
2	A Comparison of Simulated and Observed Wildfire Data.....	6
3	Wildfire Flights for the 1992 STORM-FEST Experiment	9
4	HIS Characteristics	14
5	Difference Between Wildfire and HIS Data	19
6	Difference Between Wildfire and Modified HIS Data for Water Scene.....	21
7	Difference Between Wildfire and Modified HIS Data on West-Bound Leg	21
8	Difference Between Wildfire and Modified HIS Data on East-Bound Leg	21

LIST OF ILLUSTRATIONS

No.	Title	Page
1	Simulated infrared spectrum for February 25, 1992.....	4
2	Calibrated scene data in Wildfire infrared channels.....	8
3	ER-2 flight tracks for two selected flights.....	10
4	Wildfire and HIS scan geometry from the ER-2 platform.....	12

LIST OF ACRONYMS

AOCI	Airborne Ocean Color Imager
CLASS	Cross-chain Loran Atmospheric Sounding System
EOS	Earth Observing System
FASCOD2	Fast Atmospheric Signature CODE Version 2
HIS	High-Resolution Interferometer Sounder
MAS	MODIS Airborne Simulator
MAMS	Multispectral Atmospheric Mapping Sensor
MODIS	MODerate Resolution Imaging Spectrometer
NASA	National Aeronautics and Space Administration
NCAR	National Center for Atmospheric Research
SBIR	Small Business Innovative Research
STORM-FEST	STORM-Fronts Experiment Systems Test
TOMS	Total Ozone Mapping Spectrometer
TMS	Thematic Mapper Simulator

TECHNICAL MEMORANDUM

INTER-COMPARISON OF WILDFIRE AND HIGH-RESOLUTION INTERFEROMETER SOUNDER (HIS) DATA FROM STORM-FEST: AN INVESTIGATION OF WILDFIRE SPECTRAL CHANNEL DISCREPANCIES

I. INTRODUCTION

Early in 1992, NASA participated in an inter-agency field program called STORM-FEST. The STORM-Fronts Experiment Systems Test (STORM-FEST) was designed to test various systems critical to the success of STORM I in a very focused experiment (NCAR, 1992). NASA's role in STORM-FEST was one of collecting aircraft remote sensing measurements during the field phase of the program and to participate in research supporting the use of these measurements to address specific STORM-FEST objectives.

A NASA ER-2 high-altitude aircraft was used with a suite of advanced visible, infrared, and microwave instruments to measure temperature, humidity, ozone, precipitation, and atmospheric electric fields. These instruments were used to demonstrate prototype observing capabilities and to study the structure and dynamics of winter storms and mesoscale events. Analysis of data from the Wildfire spectrometer on the ER-2 led to some uncertainty in its performance since the observations were inconsistent with the expected theoretical (modeled) results. This report describes this uncertainty and the use of the High-Resolution Interferometer Sounder (HIS) data collected simultaneously with the Wildfire spectrometer to quantify the problem.

A. Motivation for the Report

The newly developed Wildfire spectrometer (Daedalus Enterprises, Inc. under a NASA Ames Research Center SBIR) was flown aboard the NASA ER-2 to collect a variety of unique high-resolution measurements in support of STORM-FEST. This instrument was the precursor to the MODIS Airborne Simulator (MAS) which is now used in a variety of EOS funded investigations (King and Herring, 1993). During the conversion of the Wildfire to the MAS, changes to the diffraction gratings, pre-amplifiers, and associated optics and electronics packages were made after STORM-FEST. This made the Wildfire configuration obsolete.

A description of the spectral characteristics of the Wildfire is presented in Table 1. The primary Wildfire objective for STORM-FEST was to collect upwelling radiation in the channels which spanned the thermal infrared window region of the Earth's emission spectrum from 8-13 μm to detect integrated water vapor and ozone. Of particular interest were data in the 9.6 μm ozone absorption region which was sampled in the 9.2, 9.6, and 10.0 μm bands. Figure 1 presents the infrared spectrum simulated from rawinsonde data stationed at Seneca, Kansas on February 25, 1992, at 2005 UTC. Fast Atmospheric Signature CODE Version 2 - FASCOD2 (Clough et al., 1986) was used to produce the radiance spectrum (top) for the infrared window region. Brightness temperatures (bottom) were obtained from the inverse Planck function using appropriate wavenumbers. Temperature and moisture data were utilized from the special release Cross-Chain Loran Atmospheric Sounding System (CLASS) sounding. Appropriate values for surface skin temperature ($T_s = 287 \text{ K}$) and surface emissivity ($\epsilon = 0.98$) were used so that simulated window channel (band 11) brightness temperatures would approximate the observed values. In the absence of ozone profile data, the standard atmosphere climatological ozone vertical distribution (mid-latitude winter) was used with the total column ozone amount constrained by the Total Ozone Mapping Spectrometer (TOMS) retrieved value (335 D.U., taken over central Kansas). Radiative transfer calculations were made only up to the aircraft altitude (which included about 40% of the total ozone content). The radiance plot in Fig. 1 indicates that the ozone spectral signature at 9.6 μm ($1000\text{-}1070 \text{ cm}^{-1}$) is the dominate feature. Water vapor continuum absorption is responsible for the reduced upwelling radiation in the 12 μm ($900\text{-}770 \text{ cm}^{-1}$) region and is most apparent in the brightness temperature plot. Absorption by carbon dioxide is prevalent beyond 13 μm (770 cm^{-1}) but a significant feature does exist around 12.6 μm (800 cm^{-1}). Water vapor line absorption is also scattered throughout the window region. This radiative transfer modeling indicates that the Wildfire channels 8-10 (with response curves indicated by the solid triangular regions in Fig. 1) should exhibit differential absorption due to ozone with the strongest absorption occurring in the 9.6 μm band (channel 10) and decreasing in strength from the 10.0 μm band (channel 9) to the 9.2 μm band (channel 8), respectively. This difference is substantial and should be readily apparent in the observed Wildfire data. Channels 11 and 12 are differentially affected by water vapor and carbon dioxide absorption which should likewise be detected in the observed data.

The differential absorption of ozone in the Wildfire channels was the basis for applying a physical split window retrieval technique for total integrated column ozone below the aircraft [see Jedlovec and Carlson (1993) for additional research objectives]. Preliminary application of this retrieval algorithm to observed data for STORM-FEST produced results inconsistent with theoretical principles. Analysis of the problem indicated that while the 9.6 μm band was most

affected by ozone absorption (as expected from Fig. 1), the 9.2 μm band showed enhanced sensitivity to ozone content, and the 10.0 μm band was virtually insensitive to total ozone burden. This discrepancy lead to the erroneous retrieval results. A detailed investigation of the Wildfire infrared channel data is described below. The findings presented in this report have significant bearing on future use of the MAS because of its similarities to the original Wildfire configuration.

Table 1. Selected Wildfire Channels for STORM-FEST

Channel	Band Width (μm)	Central Wavelength	Constituent/Use
1	-	-	Bit bucket for channels 9-12 lsb's
2	0.675 - 0.685	0.68	Broad band visible-near infrared
3	1.605 - 1.655	1.64	Reflective infrared
4	1.955 - 2.005	1.98	Reflective infrared
5	3.675 - 3.825	3.75	Bad dewar, no data
6	4.325 - 4.575	4.50	Bad dewar, no data
7	4.575 - 4.725	4.65	Bad dewar, no data
8	9.0 - 9.4	9.20	Ozone absorption (weak)
9	9.8 - 10.2	10.00	Ozone absorption (weak)
10	9.4 - 9.8	9.60	Ozone absorption (strong)
11	10.7 - 11.2	10.95	Clean window
12	12.2 - 12.7	12.45	Water vapor (weak)
Scan Rate			6.25 rps
Instantaneous Field of View (ifov)			2.5 mrad
@20 km agl			50 m
Total Field of View (fov)			86°
@20 km agl			37.2 km
Roll Correction			±15°
Calibration			2 controlled blackbodies
Digitization			8 bit (ch's 1-8), 10 bit (ch's 9-12)
Pixels per Scan Line			716
Pixel Overlap Across Track			0%
Along Track			33%

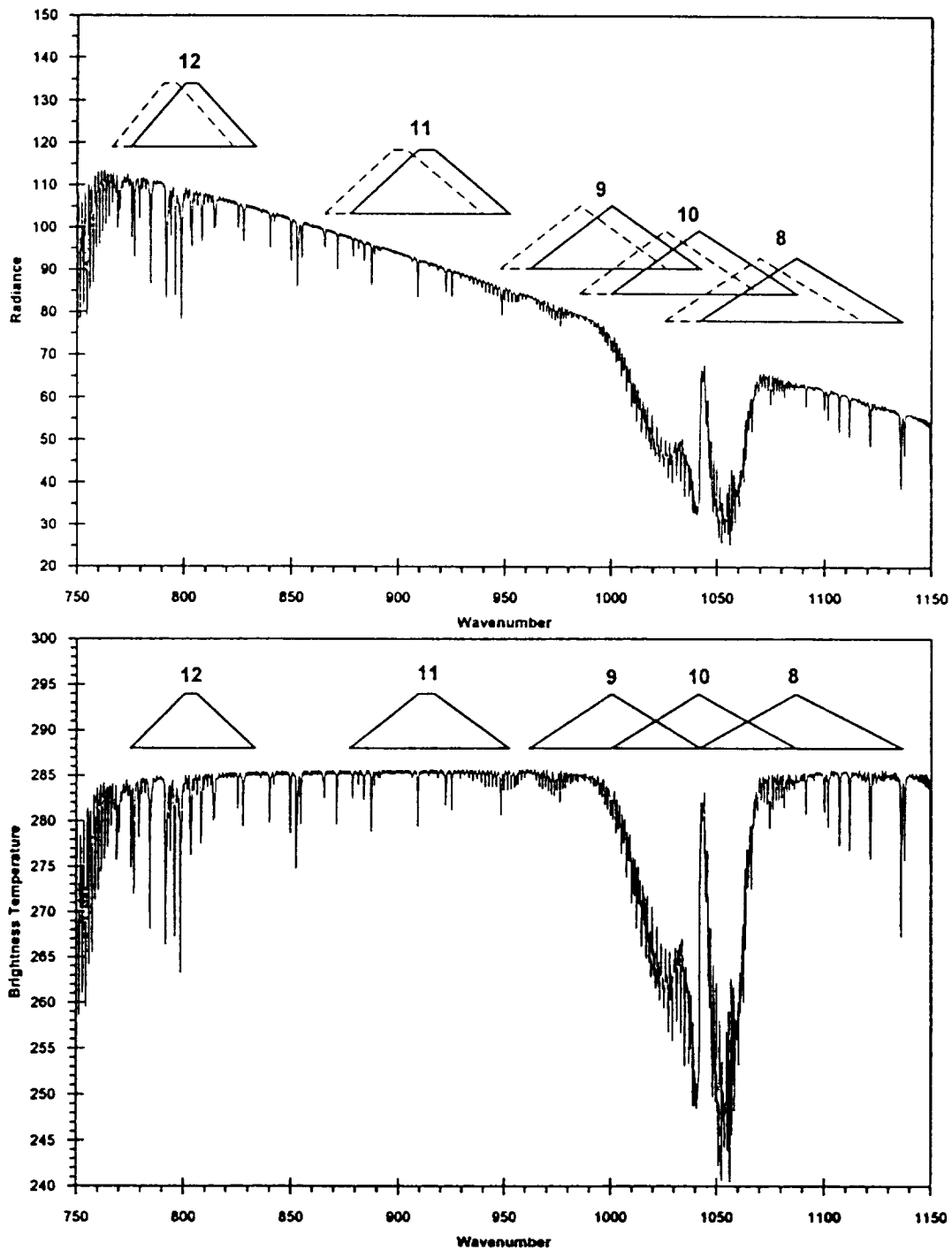


Figure 1. Simulated infrared radiance (top) and brightness temperature (bottom) spectrum on February 25, 1992. Original Wildfire spectral response curves (solid lines) are presented to indicate the band widths for each channel. The corrected response functions deduced from this study are also shown (dashed) on the radiance plot. Radiances are reported in $\text{mW}\cdot\text{m}^{-2}\cdot\text{st}^{-1}\cdot(\text{cm}^{-1})^{-1}$ and brightness temperature is in K. Wavenumbers are in cm^{-1} .

B. Understanding the Data and the Problem

Uncertainty in the Wildfire data collected during the STORM-FEST deployment led to a more robust examination of the data after the experiment. In order to address the problem, a number of questions were raised.

- Did any special atmospheric conditions exist which could explain this occurrence?
- The conversion from radiance to brightness temperature involves developing wavenumber information which is dependent on the spectral response curves of the Wildfire channels. Could the Wildfire calibration procedures be in error?
- Were the spectral response curves correct?
- Were there any problems with the instrument hardware that could contribute to these erroneous results?

The first issue is addressed below while the others are discussed in the following sections. In section II additional background material is presented on the instruments and the aircraft flights. In section III a comparison of HIS and Wildfire data is made. A likely explanation for the problem is discussed in section IV.

In an attempt to better understand and explain the observations, Wildfire channel data were simulated to reproduce the channel observations for absolute channel brightness temperatures comparison and to study relative variations between channels. The simulated spectrum for February 25, 1992 (presented in Fig. 1), was convoluted with the Wildfire spectral response values (solid band widths in Fig. 1) to produce simulated Wildfire channel data. These simulated Wildfire channel brightness temperatures are presented in Table 2. The simulated channel values are consistent with the qualitative interpretation drawn from Fig. 1. The Wildfire 9.6 μm band (channel 10) exhibits the strongest absorption, with the 10.0 μm (channel 9) band being the second strongest absorbing band. The 9.2 μm band (channel 8) is actually the warmest ozone channel indicating that it is sensing radiation in the most transparent (to ozone) region of the spectrum. The 10.95 μm band (channel 11) is the warmest of the five because it is positioned in a relatively "clean" portion of the infrared spectrum between the ozone and water vapor absorption regions. Despite the relatively small amount of moisture over the region (in the sounding), the 12.45 μm band (channel 12) is slightly colder the clean channel as a result of the water vapor absorption.

In order to highlight the problem, a direct comparison between simulated and observed channel brightness temperatures was made. Observed Wildfire data were taken from a region in northern Kansas. In order to eliminate fluctuations imposed by the variable skin temperature in the region, Wildfire data were averaged over a 24 by 40 pixel (1.2 by 2.0 km) region. A total of 38 individual Wildfire regions were selected and averaged together to obtain a mean over the area. These average observed channel values are presented along with the simulated values in Table 2. Large absolute discrepancies exist between the simulated and observed values (4-5 K) for the ozone channels. The differences are not constant in magnitude and change sign between the channels. While the 9.6 μm channel is still the coldest, the 10.00 μm channel is virtually insensitive to ozone. This is in contrast with the simulated results where the 10.00 μm channel is the second strongest ozone absorbing channel of the three. The longer wavelength channels indicate good agreement. This is partially the result of the use of an appropriate skin temperature since the atmospheric effect is rather small but also shows consistency in the comparison approach. Under the assumption that the atmosphere is homogeneous over the limited region of the data (a very good assumption for ozone), the affect of temporal or spatial misalignments should not be a factor in these discrepancies. It is also apparent that an inconsistency occurs between the channels themselves as shown in the last columns of Table 2. Differences between adjacent channels (in the spectral domain) are quite large and vary between the simulated and observed data. This apparent relative error in the observations highlights the data problem.

Table 2. A Comparison of Simulated and Observed Wildfire Data for February 25, 1992. Simulated Data are from CLASS Sonde Data at a Similar Time to the Wildfire Observations.

Channel Number	Central λ	Simulated T_{bb} (K)	Observed T_{bb} (K)	Obs.-Sim. T_{bb} (K)	Channel Difference (K)		
						Sim.	Obs.
8	9.20	281.3	276.0	-5.3			
10	9.60	265.2	269.6	4.4	8 - 10	16.1	6.4
9	10.00	278.3	283.8	5.5	10 - 9	-13.1	-14.4
11	10.95	285.1	285.2	0.1	9 - 11	-6.8	-1.4
12	12.45	282.7	282.6	-0.1	11 - 12	2.4	2.6
$T_S = 287 \text{ K}, \quad \varepsilon = 0.98, \quad O_3 = 335 \text{ D.U. (154 D.U. below 20 km)}$							

This relative bias and data problem is apparent throughout the data. Figure 2 presents Wildfire infrared channel data for a 3-minute period over Kansas on February 25, 1992, nearly simultaneous with the CLASS sonde observations. The five infrared channels of Wildfire are presented side-by-side for the same region. The images have been calibrated using standard procedures (discussed in next section). The calibrated brightness temperatures were stretched over the same range for display so that inter-channel comparisons could be visually made. Cold temperatures are portrayed as bright while warm temperatures are dark. In the infrared window region, absorption due to water vapor (in the lower layers) and ozone (in the upper layers) attenuates upwelling surface emission. Emission from ozone and water vapor is relatively small compared to surface emission. As a result, channels most sensitive to ozone and water vapor should be cold (bright) and those least sensitive to absorption should be warmest (dark). From radiative transfer theory (described above), the Wildfire 9.6 μm band (channel 10) should be coldest (brightest) with the 11.0 μm band (channel 11) being the warmest (darkest). The ozone absorption channels should range from cold (bright) to warm (dark) for the 9.6, 10.0, and 9.2 μm bands (channels 10, 9, 8), respectively. This is not the case presented in the Fig. 2. The 10.0 μm band (channel 9) is much warmer (darker) than the 9.2 μm band (channel 10) and much warmer than expected (by about 5 K) and is one of the warmest channels in the window region. This implies that the 10.0 μm band senses the least amount of constituent absorption. Similarly, the 9.2 μm band (channel 8) is colder than expected (by about 5 K) from the simulations (Table 2) and may be sensing more ozone absorption than the theory would lead one to believe. This discrepancy with the radiative transfer theory (shown in Fig. 1 and Table 2) is the crux of the problem!

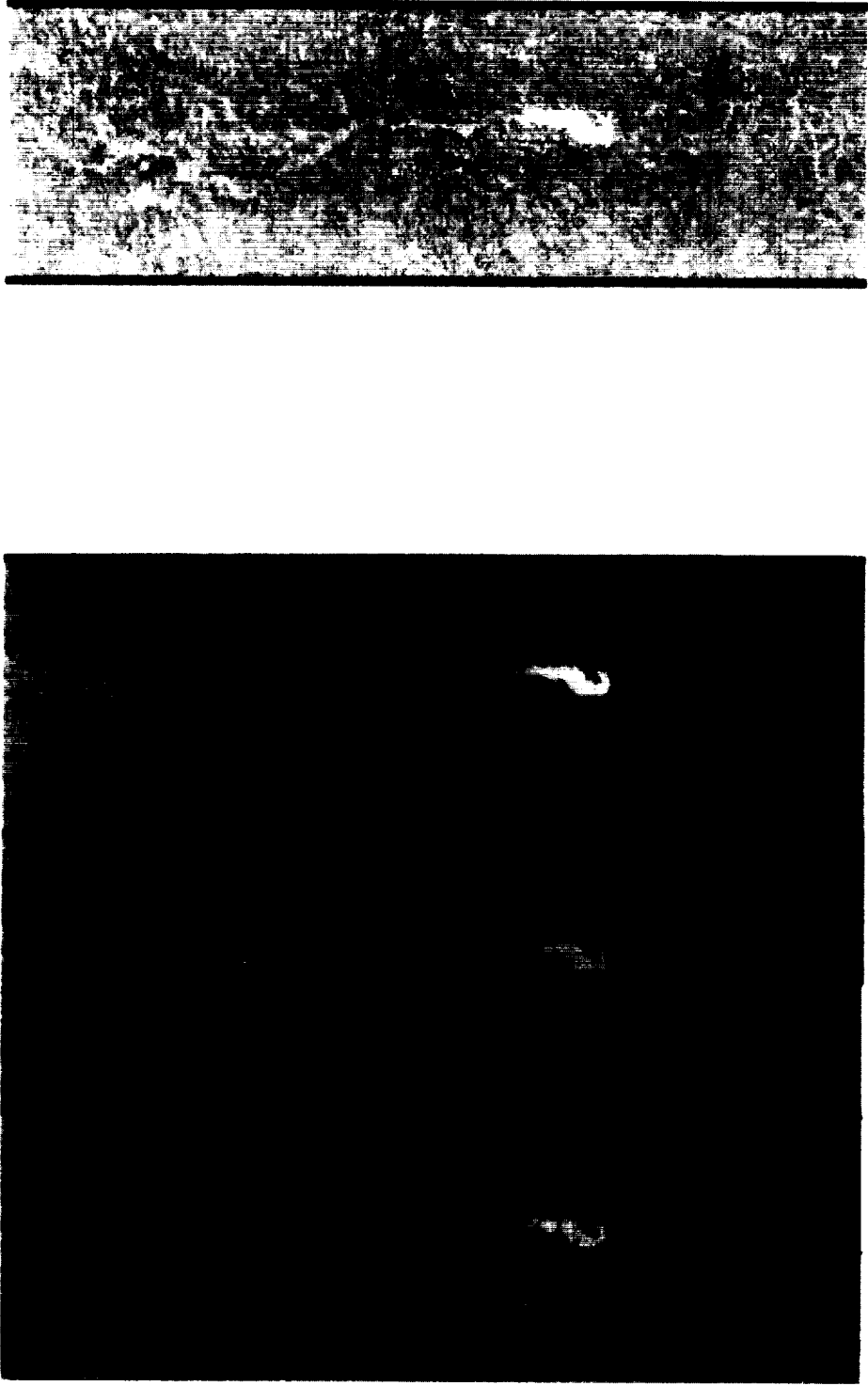


Figure 2. Calibrated scene data in Wildfire infrared channels from 2107-2112 UTC on February 25, 1992.

II. AIRCRAFT FLIGHTS AND INSTRUMENTATION

Before inter-comparison between Wildfire and HIS data are made, it is necessary to understand a bit more about the two instruments and the ER-2 observing platform. This information is presented below.

A. ER-2 Flights for STORM-FEST

The NASA ER-2 aircraft flew in support of the STORM-FEST field program from February 13 through March 15, 1992. The plane was deployed out of Ellington Field, just south of Houston, Texas. A total of 11 flights were made during the deployment, 8 of which directly supported the STORM-FEST objectives. The first five of these flights were made with the Wildfire spectrometer onboard. The remaining flights used another spectrometer (Jedlovec and Carlson, 1993). Table 3 lists details of the Wildfire flights from STORM-FEST. Two of the flights with the Wildfire spectrometer (February 14 and 17) were in direct support of the ozone variability objectives. The Wildfire spectrometer was also flown on three other supporting missions. Only the latter four flights included the HIS; however, HIS data from the February 17 flight were unusable. Extensive cloud cover reduced the useful flight data down to selected regions of flights 3 and 5. Figure 3 shows the precise location and times of the aircraft flight tracks during the two specific missions. The times indicate the period for which Wildfire and HIS data were used (1845-1905 UTC and 2140-2200 UTC on February 21 and 2033-2039 UTC, 2051-2058 UTC, and around 2107 UTC on February 25).

Table 3. Wildfire Flights for the 1992 STORM-FEST Experiment

Flight	Date	Number	Time (UTC)	Objective
1	14 Feb 92045	92061	1901-0016	Ozone variability, tropopause fold, <i>no HIS data</i>
2	17 Feb 92048	92062	2033-0326	Ozone variability, tropopause fold, <i>no HIS data</i>
3	21 Feb 92052	92063	1819-2311	Support thunderstorm flight
4	23 Feb 92054	92064	1800-0029	Support of Precipitation Mission
5	25 Feb 92056	92065	1758-0037	Support HIS moisture flight

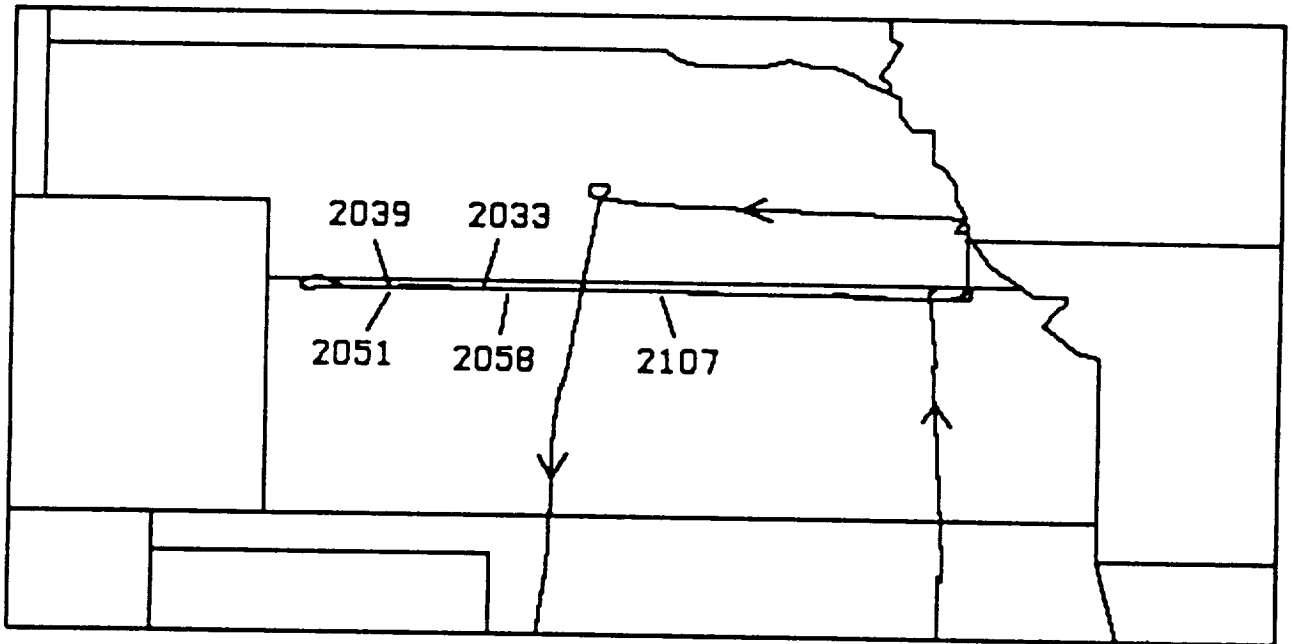
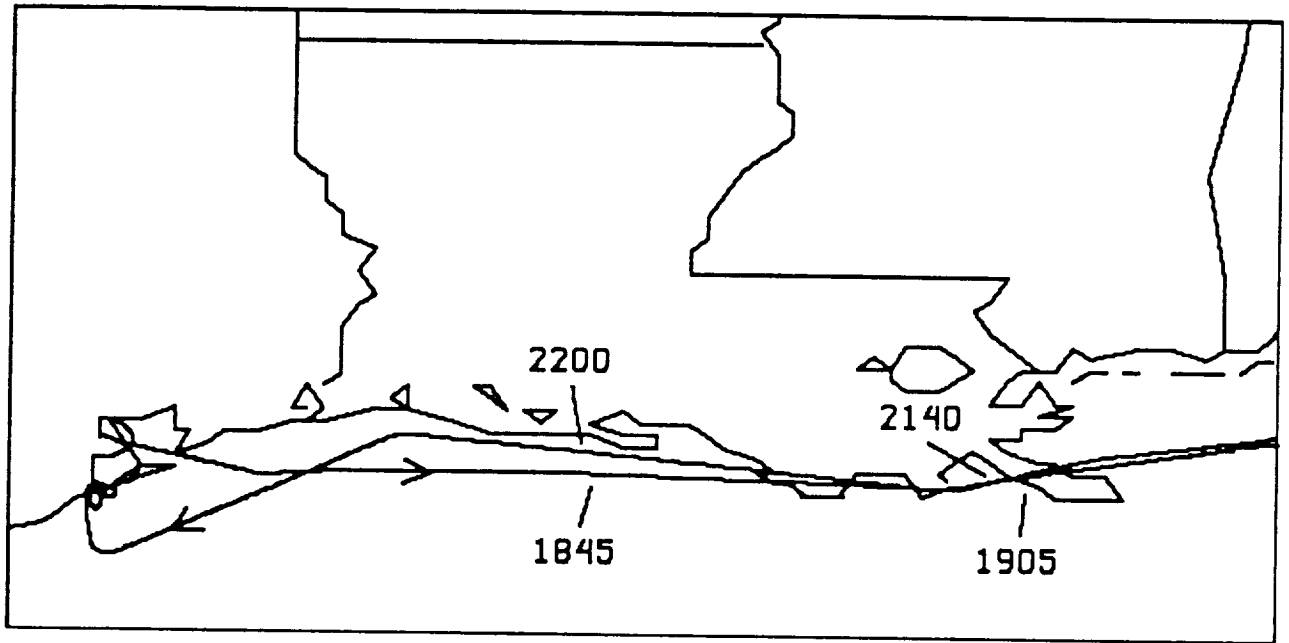


Figure 3. ER-2 flight tracks for two selected flights during STORM-FEST. The top plot is from February 21 and the bottom plot from February 25, 1992. Times on the flight tracks correspond to the data regions used in the analysis (see text for specific details).

B. Wildfire

The Wildfire spectrometer was a 50-channel airborne scanner that sensed reflected and upwelling radiation from the Earth and atmosphere in fairly narrow, uniformly spaced regions of the visible, near-infrared, and thermal infrared spectrum (from 1.17 to 12.4 μm). The Wildfire was flown on a NASA ER-2 high-altitude aircraft at a nominal altitude of 20 km during STORM-FEST, providing a horizontal ground resolution of each field-of-view of about 50 m at nadir (Table 1). The instrument scan geometry is presented in Fig. 4. From this altitude, the width of the entire cross path field-of-view scanned by the sensor is roughly 37 km, thereby providing detailed resolution of atmospheric and surface features across the swath width and along the aircraft flight track.

The Wildfire design was based on that of other instruments developed by Daedalus Enterprises, Inc. for visible and infrared mapping. It shared the same scan head, digitizer, tape system, and supporting electronics as other airborne scanners for the ER-2. The main difference between the airborne scanners is in the individual spectrometers that define the different spectral capabilities. The Wildfire channels used during STORM-FEST were presented in Table 1. These were a subset of some 43 channels which were available in the modified Wildfire configuration (also called the MODIS FIRE configuration) (King, 1991; Brown et al., 1992). As mentioned above, the primary channels of interest are the thermal infrared channels (numbers 8-12). These channels have varying sensitivity to water vapor and ozone absorption and are used to retrieve total ozone and water vapor content in the column of the atmosphere below the aircraft. The horizontal distribution of this parameter across the scan and along the aircraft flight track provides the basis for spatial analysis of these variables. The visible channels serve to identify surface and cloud features in the scene. The mid-infrared channels became unusable because of a leak which developed in the dewar. Channel 1 was used as a bit bucket for the least significant bits (9 and 10) of the 10-bit digitized data of channels 9-12 (Jedlovec et al., 1989).

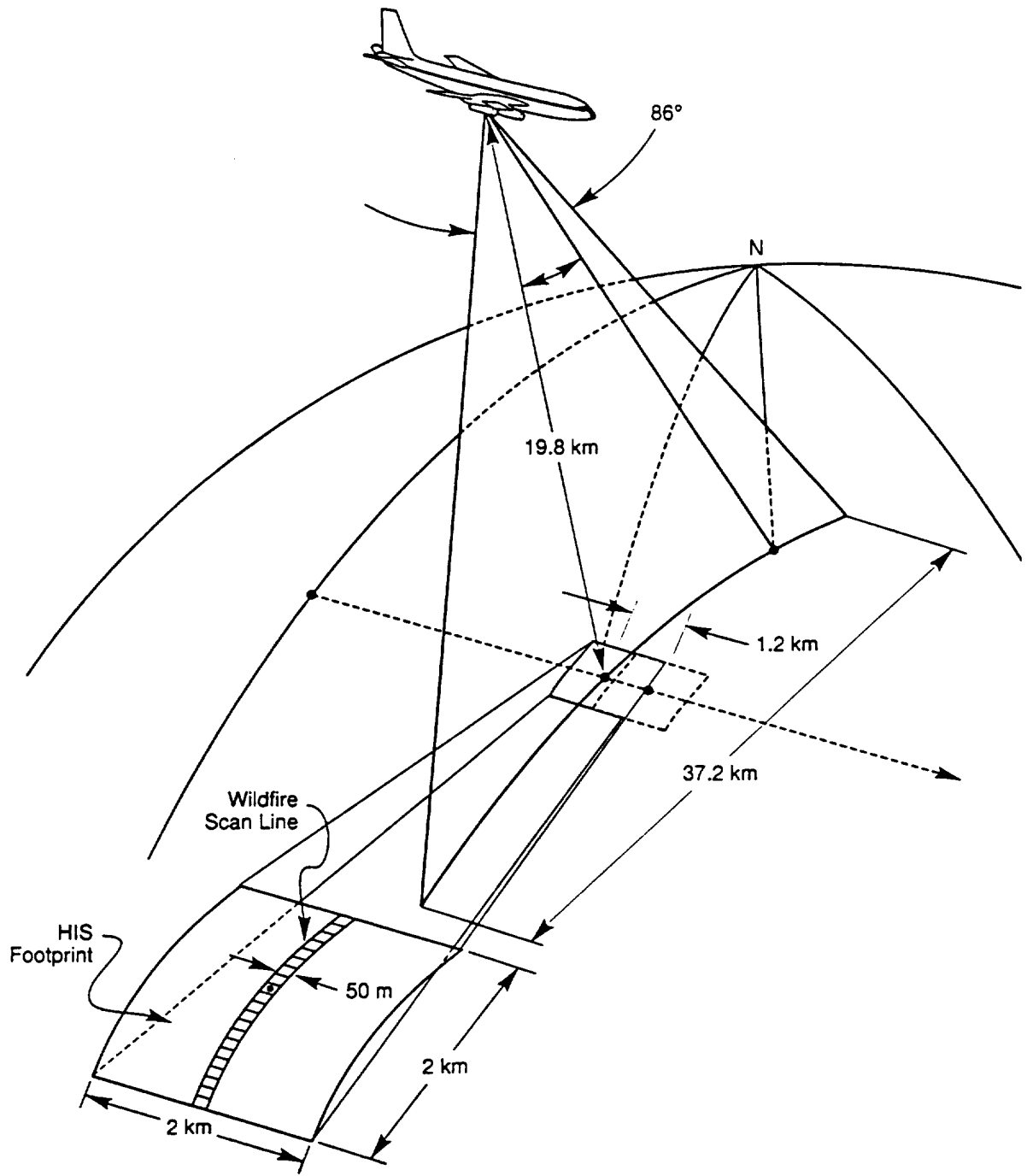


Figure 4. Wildfire and HIS scan geometry from the ER-2 platform.

C. High-Resolution Interferometer Sounder (HIS)

The High-Resolution Interferometer Sounder (HIS) is an interferometer flown on the NASA ER-2 and observes the upwelling radiance from the Earth and atmosphere in the spectral region covering from the 3.8-16.6 μm region (Smith et al., 1990). Some characteristics of the HIS are presented in Table 4. Measurements are made in three separate spectral bands with three sets of bandpass filters, focusing optics, and arsenic doped detectors in a single cooled dewar. The gain of each channel is fixed and the signals are digitized with 16-bit quantization. The raw data collected from each detector/fovs appear as a double-sided interferogram (signal formed by the recombination of out-of-phase beams of energy). Each interferogram (whether from a Earth or calibration scene) is converted to a radiance spectrum through a Fourier transform in post processing.

The HIS is a non-scanning nadir viewing instrument. Based on a 100 mrad ffov, the ground resolution of each HIS observation is 2 km (from a nominal ER-2 altitude of 20 km). An interferogram is collected every 6 seconds, corresponding to about a 1.2 km spacing (based on an ER-2 ground speed of about 208 ms^{-1}) between measurements. The HIS ffov is shown in Fig. 4 with the MAMS scan geometry. The collection of 12 samples (interferograms) of data (about 72 seconds) is usually followed by 8 samples (48 seconds) of calibration data (when scene data are unavailable). The interferograms from each scene are converted to radiance spectra, are usually co-added and are averaged to produce more reliable data. The noise equivalent delta temperature ($\text{NE}\Delta\text{T}$) and relative calibration accuracy for averaged scenes are both typically about 0.1-0.2 K over much of the spectrum (Smith and Frey, 1990). In this investigation, data from individual HIS spectra were used to precisely match the Wildfire data region. As a result, about 960 Wildfire ffov's (24 x 40 50 m pixels) are contained in each HIS footprint (see Fig. 4).

Table 4. HIS Characteristics

Spectral Range	Band I	590 - 1070 cm^{-1}
	Band II	1040 - 1930 cm^{-1}
	Band III	2070 - 2750 cm^{-1}
Instantaneous Field of View (ifov)		100 mrad
@20 km agl		2.0 km
Calibration		2 controlled blackbodies
Digitization		16 bit
Mirror Scan Rate		0.6-1.0 cm s^{-1}
Sampling rate (# contiguous Earth scenes)		6 seconds (12)
Calibration Rate (# contiguous calib. scenes)		6 seconds (8)

D. Calibration of Wildfire Data

The Wildfire detects energy from the Earth and atmosphere which is incident on the scan mirror. This spectral information is directed into the optical path of the instrument and gets convoluted by the response characteristics of the optics and band-defining filters. The spectral response characteristics of the instrument to incident energy was measured in the laboratory before delivery to Ames Research Center. These "spectral response curves" were made available to the authors for the Wildfire spectrometer by the instrument manufacturer and are the basis for the position and bandwidths presented in Table 1 and Figure 2. Unfortunately, the response characteristics were measured at only a few points for each channel. A triangular shape function and symmetry around the central value was assumed. This assumption is not inappropriate since instrument response functions tend to be symmetric and gaussian in shape. The inverse Planck function requires a single frequency in the conversion to temperature. For an asymmetric response function, the half power wavenumber (wavelength) is determined via integration of the response curve as in Jedlovec et al. (1989). For symmetric response functions the central wavenumber very nearly becomes the half power wavenumber.

Wildfire data are calibrated using procedures consistent with other Daedalus scanners and described by Jedlovec et al. (1986, 1989). A warm and cold blackbody is viewed in each

infrared channel at the beginning and end of each scan (6.25 times per second). Count values corresponding to the blackbodies are used to generate calibration curves which are highly linear in the radiance domain (radiance versus raw count value) for each infrared channel. These curves are calculated on a scan line-by-scan line basis and used to calibrate the scene data (convert raw values to radiances). The scene radiances are converted to brightness temperatures with the inverse Planck function, using the appropriate "half power" wavenumbers developed from the channel spectral response curves. Occasionally, line-to-line variations are the result of the changing calibration but were not a significant problem for these flights.

In this research investigation, an obvious question arose as to the accuracy of the spectral response functions for Wildfire. Inaccurate response functions could contribute to mis-calibration of the scene data through the use of an erroneous half power wavenumber. After talking with Daedalus (Steve Cech and Fred Osterwisch, personal communication) the authors have reasonable confidence in the limited data points for each curve (maximum response and 50% response points) and in the general symmetry or shape of the curves. [Trials in which the shape and position of the Wildfire spectral response functions were changed (and therefore different half power wavenumbers were used) showed little change in calibrated channel values.] As a result, the spectral response functions defined by the few reliable points for each band seem sufficient to calibrate the scene data and to make channel inter-comparisons. Unrealistic shapes for the response curves would be required to account for the observed channel characteristics from a calibration standpoint alone.

Because of the above, instrument calibration procedures were ruled out as a possible explanation for the channel discrepancies. However, uncertain instrument response characteristics will allow for the collection of data at wavelengths other than those desired and could significantly affect the expected results. Based on the data comparison in Table 2 and the discussion above, it was postulated that the affect of uncertain instrument response could be the cause of the brightness temperature error. It was determined that the best way to address this problem was to use the HIS spectral information collected simultaneously with the Wildfire data to form the basis for a comparison of the Wildfire accuracy. The HIS data have advantages over simulated data in that they are collected simultaneously from the same observation platform with the Wildfire data viewing the same surface and through the same atmosphere. The spectral coverage of the HIS overlaps the Wildfire channels so complete channel simulations can be made. The Wildfire response curves can be used to synthesize Wildfire data from the HIS spectrum. A direct comparison could be made for a number of points from each instrument. The methodology and results are presented in the next section.

III. DATA COMPARISON

A. Wildfire and HIS Data

The key to the HIS-Wildfire data inter-comparison lies in the ability to obtain collocated cloud-free data co-incident in both time and space. Since both instruments collected data simultaneously for a number of flights during STORM-FEST, one would think this would be an easy task. Unfortunately HIS instrument problems and clouds eliminated 95% of the data for the five Wildfire flights (plus an engineering flight and the ferry flight to Houston). From these data, portions of two aircraft flights were identified as suitable periods for the comparison. These time periods included data from 2140-2200 UTC on February 21 and from 2030-2100 UTC on February 25, 1992.

Wildfire and HIS data were collected on February 21 (flight 92063) in support of a thunderstorm mission. The flight consisted of an east-west track from Ellington Field to Tallahassee, Florida, and return (see Fig. 3 and Table 3). Although cloudy skies dominated the mission, some clear segments of flight track existed over the Gulf. During both the out-bound and return legs the ER-2 passed over the northern coastal waters of the Gulf of Mexico. Preliminary inspection of the Wildfire visible and infrared data indicated that the skies were overcast throughout the flight except for a small region where the aircraft crossed the coastline at the Mississippi River delta in southeastern Louisiana. The ER-2 overflew this area at about 1855 UTC on the east-bound leg, and again at roughly 2150 UTC on the return west-bound leg. HIS data were accordingly obtained for the 1845-1905 and 2140-2200 UTC time periods. The watery background provided a relatively uniform thermal scene, which would minimize the effect of small residual co-registration discrepancies between the Wildfire and HIS measurements.

Wildfire and HIS data were also collected on February 25 (flight 92065) in support of a ER-2 HIS water vapor sounding mission. The aircraft was dispatched to the Seneca, Kansas area where a ground-based upward-looking HIS instrument was in place, and a network of special hourly rawinsonde releases was activated. Two east-west tracks were flown along the Kansas-Nebraska border, followed by a westward leg further to the north, in southeastern Nebraska (see Fig. 3). Two segments were selected during which the ER-2 overflew the same location near the Kansas-Nebraska border, but in opposite directions; westbound at 2035 UTC, and eastbound at 2055 UTC (times are nominal). Widely scattered cumulus were occasionally present but did not interfere with evaluation of the data. The ER-2 HIS data were obtained for the two time periods (2033-2039 and 2051-2058 UTC).

The Wildfire data collected for these times appeared to be noise-free but contained the brightness temperature discrepancies previously noted. Occasionally a few missing scan lines were found, which were replaced by simple interpolation based upon neighboring existing lines of data. This was considered to be an acceptable solution because of the observed lack of radiance variability within the selected portions of the Wildfire image. Jedlovec and Carlson (1993) estimated typical NE Δ T values for the five infrared channels from these flights to be less than 0.15 K for channels 9-11 (10-bit data), less than 0.25 K (8 bit) for channel 8, and around 0.55 K for channel 12 (10 bit). Multiple line averaging of the calibration values (9 line running average) was used to reduce line-to-line calibration variations (Jedlovec et al., 1989). The Wildfire data were navigated and Earth located as per other Daedalus scanner applications (Jedlovec et al., 1989; Jedlovec and Atkinson, 1993). Absolute navigation errors were typically less than 3 pixels (150 m). Cloudy regions were subjectively determined with visible and infrared channel data. The navigation and time tagging of the Wildfire data allowed precise collocation with the HIS data. The final step averaged Wildfire channel data over the collocated HIS footprint (a 24 x 40 pixel area).

HIS data were obtained from Bill Smith at the University of Wisconsin. Complete spectra in three bands were available for the flight periods of interest. HIS channels 2 and 3 were merged at 1080 cm⁻¹ and interpolated to a slightly finer (0.25 cm⁻¹) spectral resolution in order to form a continuous spectral coverage between 750 and 1200 cm⁻¹. Wildfire data times were used with the HIS time tags to selected appropriate HIS spectrum. Additionally, the magnitude of the HIS radiance spectrum changes as a function of time (indicating large changes in skin temperature due to inhomogeneous surface features) was matched with the Wildfire 11 μ m channel data to verify corresponding collocation of times in the each data set. We have assumed that each spectrum represents a 6-second temporal integration of the spectral radiances coming from a 2 km wide spot (at 20-km altitude) located at the aircraft nadir; it was assumed the 6 seconds is centered on the time contained in the HIS record header. The ER-2 travels about 1.2 km in 6 seconds. Individual spectra (alternating forward and backward scans) are generated at 6-second intervals for a period of about 72 seconds, followed by no data for about 48 seconds, and so on. The later constraint considerably reduced the number of data comparisons and eliminated data on the outbound leg for February 21, 1992 (the HIS was in a calibration mode when it crossed the region of interest). The HIS spectra were convoluted with the Wildfire spectral response curves to produce "simulated" Wildfire data. In this way the simulated channel radiances were assumed to represent an average radiance for the HIS geographical field-of-view. These simulated Wildfire channels will be referred to as WildHIS data in the following

discussion. The WildHIS data are compared with the area-averaged Wildfire observations in the remainder of this study.

B. Inter-Comparison Results

The comparison between WildHIS (Wildfire channels simulated from HIS spectra) and Wildfire data was made for three time periods between the two different aircraft flights. The first comparison is for an ocean scene on February 21, 1992, between 2144 and 2146 UTC. Only five cloud-free HIS spectra were available for use. Differences between the WildHIS and corresponding area-averaged Wildfire data for these locations were computed. Results for the five infrared channels are presented in the first data column of Table 5. In the table, the " ΔT " entries represent the mean brightness temperature differences, in degrees Kelvin, between the actual Wildfire observations (averaged over each HIS footprint) and the WildHIS data. Positive values denote Wildfire brightness temperatures warmer than those simulated from the HIS spectra. The 9.2 μm band differences exhibit a large negative bias which means that the Wildfire data are cooler than the HIS. There is a significant positive bias for the 9.6 and 10.0 μm bands. The clean window band at 10.95 μm (channel 11) and the water vapor band at 12.45 μm (channel 12) show a negative bias. The biases are a bit confusing at first because they are not all in the same direction or of the same magnitude. The bias trend is consistent with the comparison of simulated and observed Wildfire data shown in Table 2, however. This indicates that the HIS spectrum is a good surrogate for the simulated data (and vice versa).

The biases were further explored by comparing data from the February 25 flight. These results are presented for two different time periods in the last two data columns of Table 5. The predominately cloud-free conditions on this day provided many more collocations of the data. Similarities exist between the results from the 25th with those of the 21st. For the first time on the February 25 (2033-2039 UTC), 29 collocations were made. The results indicate a negative-positive bias pattern in the ozone channels similar to data from the 21st, with the 25th biases being somewhat greater in magnitude. The window and water vapor channels indicate an opposite (positive) bias, however. The increased magnitude of the biases may result from the differences in ozone and water vapor content below the aircraft on these two days. In fact, analysis of the TOMS data for these days indicates a 45 D.U. difference (340-295) in the total ozone content between these regions. The rawinsonde data on these days indicate a large variation in moisture as well. The results for the later time (2051-2058 UTC) on February 25 show similar ozone bias features (based on 38 collocations). The bias in channels 11 and 12

shows positive values as was the case for the February 21 data. The ozone bias pattern (cooler values in the 9.2 μm band and warmer in the other two ozone channels) is a persistent trait of not only the averaged results but of the individual comparisons as well (not shown).

Since the Wildfire and HIS data were collected simultaneously from the same observing platform, the area-averaged data will capture identical radiometric properties of the atmosphere and Earth's surface. To explain the observed differences, one must again consider the data reduction and calibration procedures, and in particular the spectral calibration of the Wildfire channels. It is assumed that the HIS provides data with highly accurate relative calibration (from one wavenumber to the next) with "worse case" absolute accuracy of 1-2 K for the overall spectrum (personal communication with Bill Smith at the University of Wisconsin). A reasonable explanation drawn from the results (especially from Table 5) is that the Wildfire spectral bands (and therefore spectral response curves) may be shifted from those measured in the laboratory!

Table 5. Difference Between Wildfire and HIS Data for Various Time Periods and Flight Days

Flight Date		February 21	February 25	February 25
Time		2140-2200 UTC	2030-2039 UTC	2051-2057 UTC
# Comparisons		5	29	38
Band	μ	$\Delta T(K)$	$\Delta T(K)$	$\Delta T(K)$
8	9.20	-4.24	-5.30	-6.37
10	9.60	1.03	2.95	1.73
9	10.00	1.86	4.57	3.34
11	10.95	-0.66	0.44	-0.85
12	12.45	-0.69	0.15	-1.13

To test this theory, the "WildHIS" data were re-synthesized with new spectral response values. The HIS spectrum for all 72 points (collocated with the observed Wildfire data) was convoluted with spectral response functions which incorporated shifts to the central wavelength. A constant shift of each channel by 0.10, 0.15, and 0.20 μm was made. The assumption that the

spectral shift (if one really existed) was constant across the 9-13 μm region was speculation. In this test, the shape of each response function was preserved; only the spectral positions of the filters were allowed to vary. The new WildHIS data for the shifted response curves were differenced with the collocated Wildfire observations as before. The results are presented for the individual comparison periods in Tables 6-8. In each table, the column labeled "Design" refers to the original response functions provided by Daedalus.

The improvement in the comparison results is astonishing! By shifting the response functions to longer wavelengths, significant improvements are present in the mean difference values in most of the channels. If the minimum channel difference (for each shift) is used as a "goodness of fit" criteria, then a shift of around 0.15 μm of each channel to longer wavelengths produces the best results. The corrected response curves corresponding to this shift are shown as dashed lines on the radiance plot in Fig 1. In all cases a shift of 0.15 μm reduces the bias in all channels to less than 1.0 K. This is probably less than the combination of all known or expected error sources resulting from the methodology (absolute calibration and comparison mismatches).

Table 6. Difference Between Wildfire and Modified HIS Data for Water Scene on February 21, 1992, Between 2140-2200 UTC Using Varied Response Curves

water		Design	+0.10 μm	+0.15 μm	+0.20 μm
Band	μ	$\Delta\text{T(K)}$	$\Delta\text{T(K)}$	$\Delta\text{T(K)}$	$\Delta\text{T(K)}$
8	9.20	-4.24	-2.03	0.63	0.97
10	9.60	1.03	0.53	0.39	1.72
9	10.00	1.86	-0.02	0.62	0.99
11	10.95	-0.66	-0.62	0.60	0.56
12	12.45	-0.69	-0.12	0.05	0.13

Table 7. Difference Between Wildfire and Modified HIS Data on West-Bound Leg Over Kansas on February 25, 1992, Between 2033-2039 UTC Using Varied Response Curves

farmland		Design	+0.10 μm	+0.15 μm	+0.20 μm
Band	μ	$\Delta\text{T(K)}$	$\Delta\text{T(K)}$	$\Delta\text{T(K)}$	$\Delta\text{T(K)}$
8	9.20	-5.30	-1.90	0.31	2.84
10	9.60	2.95	2.35	0.98	1.05
9	10.00	4.57	1.46	0.39	0.35
11	10.95	0.44	0.45	0.46	0.47
12	12.45	0.15	0.71	0.87	0.95

Table 8. Like Table 7 Except for the East-Bound Leg at 2051-2058 UTC

farmland		Design	+0.10 μm	+0.15 μm	+0.20 μm
Band	μ	$\Delta\text{T(K)}$	$\Delta\text{T(K)}$	$\Delta\text{T(K)}$	$\Delta\text{T(K)}$
8	9.20	-6.37	-3.06	-0.90	1.59
10	9.60	1.73	1.17	-0.18	-2.19
9	10.00	3.34	0.22	-0.86	-1.60
11	10.95	-0.85	-0.83	-0.82	-0.80
12	12.45	-1.13	-0.58	-0.41	-0.34

IV. CONCLUSION

The absolute and relative calibration of the Wildfire spectrometer image data has been evaluated using radiative transfer theory and simultaneous interferometer data from the HIS. Data from 79 collocated points during two different aircraft flights were used in the comparison. Results indicate large discrepancies between the HIS-derived and actual Wildfire observations. The discrepancies are spectrally dependent and may be consistent from flight to flight. Instrument calibration procedures and variations in atmospheric moisture and ozone have been ruled out as possible explanations for the results. All empirical information points to a spectral discrepancy between the (presumably) known spectral response curves and the actual spectral response of the instrument. A shift of the reported spectral response curves by 0.15 μm to longer wavelengths in all infrared channels provided a precise fit to the HIS data given the accuracy of both measurements and collocation and averaging procedures. With the shift, the measurements agree in an absolute sense to within 1.0 K in all five infrared channels.

We were not able to determine the source of the problem described above. If our assumption of the shift in instrument spectral response is correct, several explanations could be possible. Precise instrument spectral response values are not known. Although this has a limited effect on the calibration accuracy (conversion of raw counts to brightness temperatures), it could have dramatic effects on energy received by the detectors in spectral regions where atmospheric transmittance varies greatly with changing wavelength. Spectral response curve uncertainties (discrepancies from the actual or real response values) could result from erroneous laboratory measurements as well as hardware problems. The somewhat unique design of the Wildfire in which a diffraction grating is used to spectrally separate incident energy depends heavily on the position of the filter in the optical path. Unlike systems which use dichroic and/or bandpass filters exclusively to provide spectral separation and discrimination (e.g., other Daedalus airborne scanners such as the MAMS, AOCI, and the TMS), small changes in the optical position of the grating during flight (due to expansion and contraction, vibrations, etc.) could produce significant spectral shifts. Unfortunately, changes to the configuration of the Wildfire spectrometer after the STORM-FEST experiment precluded an engineering assessment of the problem.

These findings could have significant bearing on other airborne and satellite instruments under development which rely on gratings for accurate spectral separation. The Wildfire spectrometer was the precursor to the MODIS Airborne Simulator (MAS) and utilizes similar diffraction grating technology. An intercalibration of the spectral characteristics of the MAS

channels in the laboratory and during flight on the ER-2 aircraft would be appropriate and is recommended. The HIS provides an excellent benchmark for spectral calibration accuracy throughout the infrared region. Specific calibration and inter-comparison flights (if conducted) should be well controlled to eliminate uncertainties in the data comparisons.

REFERENCES

- Brown, K. S., M. King, P. Menzel, C. Moeller, and T. Arnold, 1992: Engineering evaluation of the MODIS-N airborne simulator (MAS) remote sensor performance during the FIRE campaign. Unpublished report (available from the authors).
- Clough, S. A., F. X. Kneizys, E. P. Shettle, and G. P. Anderson, 1986: Atmospheric radiance and transmittance: FASCOD2. Preprints Sixth Conference on Atmospheric Radiation, Amer. Meteor. Soc., Boston, 141-145.
- Jedlovec, G. J., and G. S. Carlson, 1993: Wildfire and MAMS data from STORM-FEST. NASA TM-108393, 31 pp. (available NTIS).
- Jedlovec, G. J., and R. J. Atkinson, 1993: Calibration, navigation, and registration of MAMS data for FIRE. NASA TM-108397, 56 pp. (available NTIS).
- Jedlovec, G. J., K. B. Batson, R. J. Atkinson, C. C. Moeller, W. P. Menzel, and M. W. James, 1989: Improved capabilities of the Multispectral Atmospheric Mapping Sensor (MAMS). NASA TM-100352, 80 pp. (available NTIS).
- Jedlovec, G. J., W. P. Menzel, R. J. Atkinson, and G. S. Wilson, 1986: The Multispectral Atmospheric Mapping Sensor (MAMS): Instrument Description, Calibration, and Data Quality. NASA TM-86565, 37 pp. (available NTIS).
- King, M., and D. Herring, 1993: The MODIS Airborne Simulator (MAS). *The Earth Observer*, 15-19.
- King, M., 1991: Status of MODIS-N Airborne Simulator (MAS). Unpublished report dated September 5, 1991 (available from the authors).
- NCAR, 1992: STORM-FEST Operations Plan. Available National Center for Atmospheric Research, P.O. Box 3000, Boulder, CO, 80307-3000, 316 pp.
- Smith, W. L., and R. Frey, 1990: On cloud altitude determinations from High-resolution Interferometer Sounder (HIS) observations. *J. Appl. Meteor.*, **29**, 658-662.
- Smith, W. L., H. E. Revercomb, H. B. Howell, H.-L. Huang, R. O. Knuteson, E. W. Koenig, D. D. LaPorte, S. Silverman, L. A. Sromovsky, and H. M. Woolf, 1990: GHIS - The GOES High-Resolution Interferometer Sounder. *J. Appl. Meteor.*, **29**, 1189-1204.

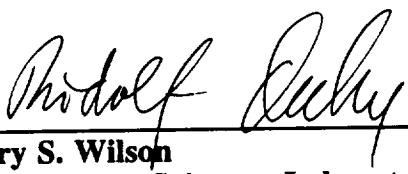
APPROVAL

**INTER-COMPARISON OF WILDFIRE AND HIGH-RESOLUTION
INTERFEROMETER SOUNDER (HIS) DATA FROM STORM-FEST:
AN INVESTIGATION OF WILDFIRE SPECTRAL CHANNEL
DISCREPANCIES**

By

G. J. Jedlovec and G. S. Carlson

This report has been reviewed for technical accuracy and contains no information concerning national security or nuclear energy activities or programs. The report, in its entirety, is unclassified.



Gregory S. Wilson
Director, Space Sciences Laboratory

